International Journal of Gas Turbine, Propulsion and Power Systems
September 2024, Volume 15, Number 5

The effect of different blade geometrical parameters on the operational flexibility and aerodynamic performance of axial sCO_2 turbines

Abdelrahman S. Abdeldayem[1], Martin T. White[2], and Abdulnaser I. Sayma[3]

[1] Centre for Propulsion and Thermal Power Engineering, School of Aerospace, Transport and Manufacturing,
Cranfield University, Bedfordshire, MK43 0AL, United Kingdom

[2] Energy and Materials Engineering Research Centre, School of Engineering and Informatics,
University of Sussex, Brighton, BN1 9RH, United Kingdom

[3] College of Engineering, Design and Physical Sciences, Brunel University, Uxbridge, London, UB8 3PH, United Kingdom

ABSTRACT

Improving the off-design performance and turndown capability of power cycles for concentrated solar power (CSP) applications is critical considering possible heat source and cooling fluctuations. In this paper, the effect of different geometric flow-path parameters on the aerodynamic performance of large-scale axial turbines operating with supercritical carbon dioxide (sCO_2) mixtures at both design and off-design conditions is evaluated. The turbine power considered for this analysis is approximately 130 MW and corresponds to a 100 MW_e CSP plant. A series of 3D steady-state multi-stage Reynolds-Averaged Navier Stokes equations Computational Fluid Dynamics (CFD) simulations are performed utilising the k-ω SST turbulence model. The number of stages, stator/rotor axial gap, leading-edge thickness, inlet wedge angle, and stagger angle are varied to evaluate their impact on the turbine operational flexibility, defined by the minimum acceptable ratio of mass flow rate to the design value. The ranges of variation are defined based on practical considerations and careful consideration of various design criteria such as the slenderness ratio and bending stresses. The results reveal that the stagger angle has the largest influence on the operational flexibility with a change of 17.1% in the minimum allowable part-load mass flow ratio corresponding to a change in the stagger angle between -5° and +5° from the reference design angle. This increase in stagger angle resulted in an increase in the design point total-to-total efficiency of 2.3 percentage points. The leading-edge thickness has the least influence with a maximum change in the minimum part load mass flow ratio of 0.63% as obtained for the investigated range, and a negligible change in the design point efficiency. Investigations of the flow field reveal that increasing the stagger angle reduces the size of separation regions caused by increased incidence, despite higher stagger angles increasing blade bending stresses.

Manuscript Received on July 25, 2023
Review Completed on August 9, 2024

KEYWORDS

Axial turbines, Computational fluid dynamics, off-design, supercritical CO_2

INTRODUCTION

The use of supercritical carbon dioxide (sCO_2) is promising for achieving high thermal efficiency in power generation cycles integrated with concentrated solar power plants (CSP) in addition to obtaining a small physical footprint [1]. Designing efficient system components is essential to reducing the levelised cost of electricity (LCoE) and turbines are considered one of the major contributors to cycle performance [2]. Evaluating turbine off-design performance is important to assess cycle performance at variable operating conditions. The off-design operation range of axial turbines is limited by the minimum allowable efficiency, or the maximum exhaust temperature that can be tolerated by the selected materials, and this is important given challenging operating conditions and the high inlet temperatures proposed for supercritical CO_2 power cycles [3].

Operating with sCO_2 introduces various technical challenges to the design process that are related to both the operating conditions as well as the properties of the working fluid. Firstly, considering that existing mean line loss models were developed and calibrated for steam and air turbines, using these models to design the flow path of axial turbines operating with sCO_2 mixtures may introduce uncertainties. Therefore, certain design assumptions, such as the stagger angle, should be verified using other means, such as 3D numerical models. Moreover, translating a preliminary mean line geometry into a suitable blade profile requires various assumptions related to the shape of the leading-edge and the stator/rotor axial gap as examples. Alongside this, the high operating pressures, the high-pressure difference across the turbine, and the compact design resulting from the high gas density of sCO_2 at the proposed operating conditions lead to high blade bending stresses. Factors such as the blade thickness and the stagger angle influence theses stresses, and therefore should be adjusted to satisfy the safety constraints. The high operating temperature also adds technical challenges associated with material compatibility, thermal stability of the working fluid, compatibility with dry gas seals as well as the design of the cooling system; however, these challenges are not directly linked to aerodynamic performance. Indirectly, the design of the thermal system may constrain the size of the flow path; for example, increasing the stator/rotor axial gap, or increasing the number of stages, increases the flow path length and impacts the rotor dynamic stability of the shaft which in turn is linked to the operating temperature and the design of interstage seals [4]. Although not specific to sCO_2, the power scale of the proposed designs also influences off-design performance. For large scale applications, only direct drive between the turbine and electrical generator can be used, requiring a fixed rotational speed that is synchronous with the grid. This can limit the off-design performance and operational flexibility of the turbine. In terms of aerodynamic performance, turbine stage performance is typically dominated by the secondary flow losses that result from the relatively short blades compared to the blade chord length [5]. One of the investigated parameters, specifically the number of stages, affects the blade aspect ratio and the secondary flow losses of the turbine stage.

The aerodynamic design of axial turbines has been widely investigated for conventional working fluids such as air compared to non-conventional working fluids such as sCO_2 mixtures, especially at off-design [6, 7]. Aerodynamic losses in sub-sonic axial turbines include tip clearance, secondary flow, profile, and trailing edge losses. At off-design operation, other sources of losses exist depending on the methodology of load control. Partial admission results in a source of loss that develops due to the uneven circumferential distribution of the mass flow rate at the inlet to the turbine. In the case of sliding pressure control, the working fluid is admitted evenly across the circumference, but change in mass-flow rate and inlet velocity means the resulting flow angles are not aligned with the blade causing increased incidence losses [8].

Various assumptions made during flow-path design can impact turbine performance at both design and off-design operating conditions. As such it is necessary to evaluate these parameters in terms of their potential to enhance turbine operational flexibility; here flexibility is defined in relation to the feasible range of mass flow rates that can be efficiently handled by a specific turbine design. Hamakhan and Korakianitis [9] investigated the influence of the leading-edge geometry on the aerodynamic performance of gas turbine blades. The results have shown that utilizing the Hodson–Dominy blade design mitigated the formation of the leading-edge separation bubbles over the tested range of incidence angles which corresponded to $\pm 10^{o}$. Benner et al. [10] indicated the possibility of reducing profile losses at higher incidence angles by increasing the leading-edge thickness and the inlet wedge angle. Dossena et al. [11] investigated the influence of the stagger angle and pitch-chord ratio of a linear cascade on secondary flows at off-design operating conditions. Measurements found that the aerodynamic performance was highly sensitive to the stagger angle which was the tested in the range of -4^{o} to $+2^{o}$.

These results demonstrate the potential to control these losses by modifying flow path design parameters. For example, larger blade aspect ratios can significantly reduce endwall losses, whereas adjustments to the blade cross-sectional geometry influence profile and incidence losses. However, such geometrical adjustments are subject to certain design constraints, such as adhering to a maximum slenderness ratio alongside bending stress limits [12]. Increasing the slenderness ratio, which represents the ratio of flow path length to mean blade diameter, beyond a certain limit may impact rotor dynamic stability while exceeding the bending stress limit could potentially lead to structural failure. Hence, a careful balance must be maintained during the aerodynamic design process to optimise design and off-design performance while ensuring structural integrity and stability.

The limits for off-design operation can be defined based on different aspects including the aerodynamic performance, the turbine exhaust temperature, the thermal stresses, and the mechanical stability of the rotor [13]. The off-design operational range is also linked to the expected operating conditions, and the specific turbine control strategy employed [14]. From a practical standpoint, the minimum part-load mass flow rate can be defined based on the maximum allowable exhaust temperature for a constant inlet total temperature. Decreasing the mass flow rate of the turbine would increase the exhaust temperature because of decreasing the pressure ratio while maintaining the same inlet temperature defined by the cycle.

In this paper, the effect of different flow path design parameters on the performance and operating range of sCO_2 axial turbines is investigated. This includes evaluating the impact of varying the number of stages, leading-edge thickness, inlet wedge angle, stator/rotor axial gap, and stagger angle, on the minimum acceptable mass flow rate at part-load operation. These design parameters are varied within a range defined based on practical considerations to show the sensitivity of the turbine operational range to each parameter. The analyses are supported by flow field investigations using CFD, showcasing the possibilities for enhancing part load performance while complying with imposed design constraints. The findings of this study provide recommendations for future design activities aiming at improving the operational flexibility of large-scale sCO_2 axial turbines for applications where variations in the operating conditions are expected. The new findings of this paper include quantifying the impact of specific design parameters on both design and off-design performance. This has led to the identification of the most dominant parameters, such as the stagger angle, which should be optimised to enhance operational flexibility and improve turbine performance across a wide range of operating conditions. It is worth reiterating that previous design practices developed for conventional steam and air turbines may not be suitable for sCO_2 turbines due to the differences in the fluid and operating conditions. For example, the findings from this study indicate that increasing the leading-edge thickness has a minor impact on the off-design performance of the examined turbine for which the inlet Reynold number exceeds 10^7. This is in contrast to previous studies that indicate that increasing the leading-edge thickness can improve aerodynamic performance of conventional gas turbines when the Reynolds number is around 3×10^5 [15].

METHODOLOGY

<u>CFD model</u>

Several CFD simulations of the turbine were performed at both design and off-design operating conditions. The flow model uses the Reynolds Averaged Navier Stokes (RANS) equations with the shear stress transport (k-ω SST) turbulence model to close the system of equations as it has been found to be the most suitable for turbomachinery applications [16]. Although the RANS models are not the most accurate in predicting the flow structure in cases of flow separation, they provide a reasonable accuracy that can fairly indicate the turbine performance at both design and off-design conditions. A single-passage, 3D, multi-stage flow domain is used as shown in Figure 1. A mixing plane approach is used at the interface between stationary and rotating flow domains, which is sufficiently accurate for the purpose of performance modelling with the least numerical instabilities compared to the frozen rotor approach in steady-state simulations [16]. The boundary and operating conditions are summarised in Table 1. The rotational speed of 3,000 RPM is fixed to meet the grid requirements for a direct drive application.

The rotor blades are unshrouded with a clearance gap equal to 0.07% of the blade tip diameter defined between the rotating shroud and the casing. The working fluid used in this study is CO_2 mixed with sulphur dioxide (SO_2) as recommended from the cycle analysis conducted as part of the SCARABEUS project [2]. The thermophysical properties of the CO_2 mixture are evaluated using the Peng Robinson equation of state coupled with a binary interaction parameter obtained via regression of experimental data [17]. It is worth noting that the selection of a suitable equation of state is most critical when the operating conditions are near the critical point. As such, there is not a large sensitivity when considering the turbine in isolation because the turbine operates away from the critical point where non-ideal effects are most significant [18]. Crespi et al. [19] examined the compressibility factor for different mixtures at turbine inlet conditions of 700 °C and 239 bar. The results for pure CO_2, a mixture of CO_2-C_6F_6 (85% - 15% by mole), and a mixture of CO_2-$TiCl_4$ (85% - 15% by mole) corresponded to compressibility factors of 1.054, 1.069, and 1.058, respectively. These results indicate that the behaviour of CO_2 mixtures at the turbine inlet closely approximates ideal gas behaviour and is less sensitive to the equation of state or binary interaction parameter. The thermophysical properties are introduced to the CFD model through tables covering the expected pressure and temperature ranges with a resolution of 500 × 500 points.

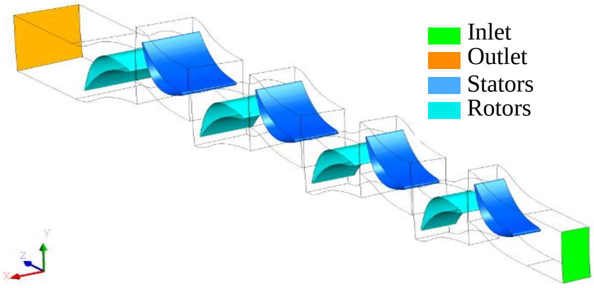

Figure 1 CFD model domain of a 4-stage design.

Table 1 Boundary and operating conditions

Design parameter	Symbol	Value
Selected dopant [-]	-	SO_2
Molar fraction [%]	z_m	20
Inlet total pressure [bar]	P_{01}	100~239
Inlet total temperature [K]	T_{01}	973
Outlet static pressure [bar]	P_e	81.24
Rotational speed [RPM]	N	3000

Grid independence study

A study has been conducted to investigate the relationship between the mesh size and the aerodynamic performance at both design and off-design operating conditions. The relation between the number of grid points and the total-to-total efficiency at the design point and at 50% of the design mass flow rate is shown in Figure 2. At the design point, the convergence of the total-to-total efficiency can be achieved using around 0.6 million grid points per stage with a tolerance as low as 0.05% relative to the finest mesh. However, the off-design operating condition requires a finer mesh structure to accurately represent the case. A total number of grid points of 2.8 million per stage is necessary to reach a tolerance in total-to-total efficiency of 0.2%. It is worth noting using the design-point mesh to simulate off-design conditions could correspond to an uncertainty in the total-to-total efficiency of up to 0.5%.

Structural analysis

Bending stresses present a major constraint during the design of sCO_2 turbines due to the compact size and high-pressure differences. Although average stresses are evaluated during the mean-line design phase [20], the location and magnitude of the maximum stress is not identified. Therefore, finite element analysis (FEA) is used to evaluate the equivalent stress distribution on the blade to identify regions of peak stress, which can be used to improve the design and ensure the factor of safety remains within acceptable limits.

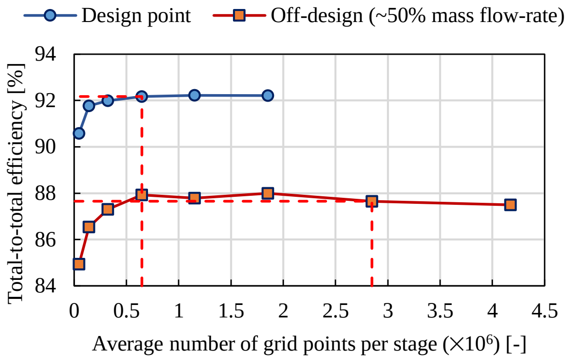

Figure 2 Results of mesh sensitivity at design and off-design for a 4-stage 130 MW design operating with CO_2-C_6F_6 mixture.

The FEA model is set up using the 3D blade geometry defined for the CFD model. The aerodynamic loads, specifically the pressure distribution on the blade walls calculated by the CFD simulations, are applied to the blade wall to define the boundary conditions for the FEA model. Additionally, the FEA model considers the centrifugal load on the rotor blades resulting from the rotation of the shaft. The blade is modelled using a fixed solid base attached to the shroud surface of the stator blade and the hub surface of the rotor blade as shown in Figure 3. The solid base is 5 mm thick with a fillet between the blade and the base to represent the physical blade geometry after manufacturing. Further details of the FEA model can be found in the authors' previous publication [21].

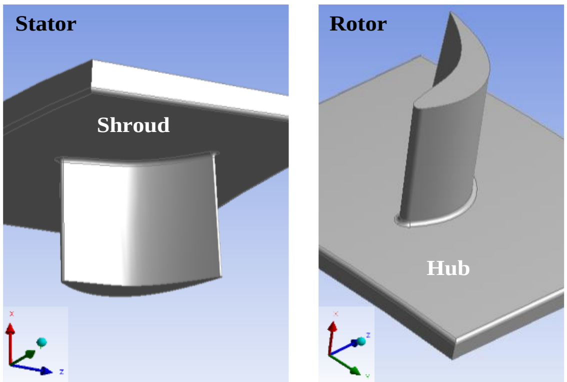

Figure 3 The stator and rotor geometries for the FEA analysis.

Model validation

The CFD setup was validated against experimental data available for a 4-stage axial air turbine that produces 703 kW power and was developed by Petrovic and Riess [22]. The turbine rotational speed is 7,500 RPM with inlet pressure, temperature, outlet pressure, and mass flow rate of 2.6 bar, 413 K, 1.022 bar, and 7.8 kg/s, respectively. The off-design performance simulations were set up using variable inlet pressure ranging between 1.15 bar to 1.45 bar which corresponds to a mass flow rate that ranges between 35% to 100% of the design mass flow rate. The results for the relationship between total-to-total pressure ratio and total-to-static efficiency are shown in **Error! Reference source not found.**, w hich compares the CFD model results to the experimental and numerical data provided by Petrovic and Riess [22] (P&R). A good agreement between the CFD model and the experimental and numerical results is achieved. The deviation in total-to-static efficiency at the design point is between 1.7% and 2.9% when compared to the experimental and numerical results respectively.

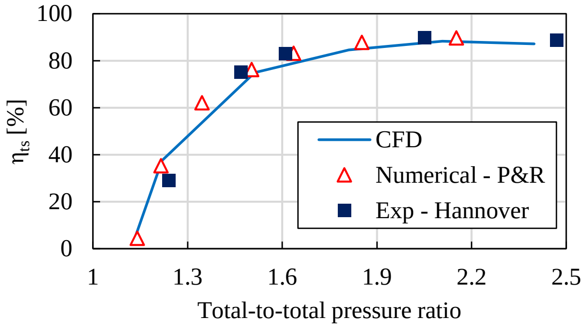

Figure 4 Total-to-static efficiency against the total-to-total pressure ratio of the verification air turbine.

DESIGN PARAMETERS

A set of flow path design parameters has been selected to evaluate their influence on the off-design performance and the turn-down capability of an axial turbine operating with a sCO_2-SO_2 mixture. These parameters include the number of stages, the stator/rotor axial gap, the blade leading-edge thickness, the blade inlet wedge angle, and the blade stagger angle. A list of the selected design parameters and their limits is reported in Table 2. These parameters have been selected based on the results of previous studies conducted by the authors, including blade shape optimisation and aerodynamic loss analysis of axial turbines operating with sCO_2 mixtures [5, 21].

The number of stages has been selected for this study based on the preliminary design investigations of the flow path which includes various assumptions such as the number of stages, number of blades, flow coefficient, loading coefficient, degree of reaction, and pitch-to-chord ratio. The number of blades was chosen to align with the bending stress limits. The flow coefficient, loading coefficient, and degree of reaction values of 0.5, 1, and 0.5 were selected based on standard optimal values for these parameters [20]. It has been found that the number of stages plays a dominant role in controlling the aerodynamic performance at the design operating conditions by varying the pressure drop per stage and the hub diameter. Consequently, the number of stages is selected for this study to assess its impact on the performance at part-load operating conditions.

Table 2 Range of variation of the selected design variables

Parameter	**Ref.**	**Min.**	**Max.**
Number of stages [-]	4	4	14
Stator/rotor axial gap to pitch ratio [%]	33	15	50
Leading-edge thickness [mm]	2.5	2.5	6
Inlet wedge angle [deg]	15	5	25
Stagger angle deviation [deg]	0	-10	+5

Several design assumptions have been made to generate the 3D blades from the mean line design results [23]. Among these assumptions, the blade shape near the leading-edge is selected for this study by varying the leading-edge thickness and the blade inlet wedge angle. These parameters are specifically selected based on the blade shape optimisation results conducted by the authors [21], which have shown that adjusting the blade thickness near the leading-edge can enhance performance in stages where incidence occurs. Furthermore, the blade shape optimisation results have shown that increasing the stagger angle can improve the aerodynamic performance despite the potential increase in the blade stresses. Ultimately, the stator/rotor axial gap is included to assess the possibility of reducing it to limit the shaft length and improve the rotor dynamic stability. This can also contribute to decreasing the shaft weight and overall cost. However, decreasing the stator/rotor axial gap impacts the mixing losses between the stages, as defined by Denton [24], particularly at part-load conditions when the flow angles are more likely to deviate from the blade angles.

The selection of the parameter ranges was made after careful consideration, taking into account recommendations from previous studies and practical considerations. These ranges have been defined to ensure that the assumptions are feasible and have minimal impact on the other aspects of the turbine design, such as shaft rotor dynamic stability and blade bending stresses. For instance, the number of stages is constrained by the slenderness ratio and the hub diameter. Increasing the number of stages beyond this range would increase the slenderness ratio and could impact the rotor dynamic stability. On the other hand, too few stages would result in larger hub diameters, potentially affecting the rotor inertia and shaft end size that have to align with the current size limitations of dry gas seals (DGS) [25]. The upper and lower limit of the stagger angle is constrained by the bending stresses and aerodynamic performance respectively. The reference stagger angle, selected for the reference design, was based on practical considerations combining mechanical design and aerodynamic performance. This stagger angle is derived as a function of the outlet blade angle, which was based on recommendations from industrial partners within the SCARABEUS project. Increasing the stagger angle to enhance aerodynamic performance is possible, but the effect on the resulting blade stresses should be considered. Conducting FEA on the blades with the new stagger angles is necessary to ensure that the structural integrity of the blades is maintained within acceptable limits. The thickness of the leading-edge is also subject to limitations, with its lower limit determined by blade bending stresses and its upper limit tied to aerodynamic performance. Increasing the blade thickness near the LE can be achieved by increasing the leading-edge thickness, or increasing the inlet wedge angle which can improve the aerodynamic performance at part-load when incidence occurs; however, this could impact design point performance by increasing blade profile losses. The stator/rotor axial gap is bounded by the slenderness ratio and weight on the upper limit and performance considerations on the lower limit. Decreasing the stator/rotor axial gap may deteriorate performance due increased mixing losses resulting from the limited distance downstream of a turbine blade row in which the wake region of the upstream blade trailing edge is allowed to dissipate.

In this study, each of the proposed design variables is varied individually to quantify its impact on the off-design performance of axial turbines operating with novel working fluids where the practical experience established for steam and air turbines may be unsuitable. As such, this study highlights the impact of adjusting each of the proposed design variables. Of course, the simultaneous adjustment of these parameters is also possible and this could be studied in future to further improve off-design performance. For example, in a previous study conducted by the authors, it was found that high incidence in the last stages of multistage turbines operating with sCO_2 mixtures can be mitigated by increasing the stagger angle, the inlet wedge angle and the inlet fillet radius simultaneously [21].

RESULTS AND DISCUSSION

The off-design operation of different turbine designs has been investigated to identify their operational flexibility and aerodynamic performance. At off-design, differences in the mass-flow rate lead to reductions in velocity and deviations in the flow angle compared to the angle of the blade. This results in an incidence loss, which is related to the incidence angle and is defined as the difference between the flow and blade angles. The incidence angle at the rotor inlet of each stage of the 4-stage turbine design is reported against the stage number for different total-to-static pressure ratios in Figure 5. The corresponding total enthalpy drop per stage is shown in Figure 6. From these figures, it can be seen that the incidence angle increases as the operating condition moves away from the design pressure ratio of 2.73, and as the stage number increases. Moreover, as the pressure ratio reduces and stage number increases the performance deteriorates, leading to very low or even negative work output. That means the tangential force on the blades of stages with high negative incidence angles could be negative resulting in stages that extract work from the shaft.

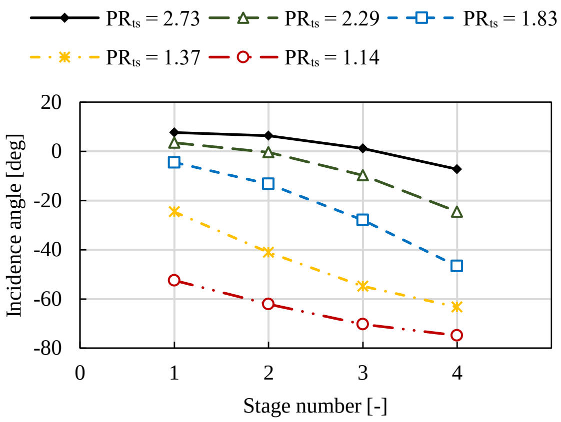

Figure 5 Incidence angle at the rotor inlet calculated for different operating conditions.

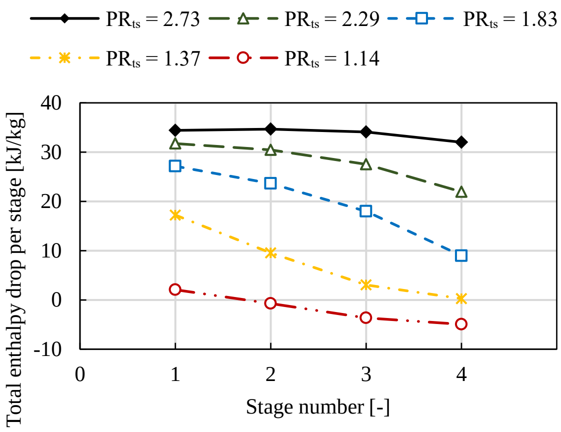

Figure 6 Total enthalpy drop per stage calculated for different operating conditions.

The off-design performance is presented in the following sections for the various flow path design parameters. In this analysis, the ratio between the mass flow rate and the design mass flow rate is introduced to represent of the flow rate through the turbine. It is important to note that the mass flow rate in this analysis is obtained by varying the inlet total pressure. This approach leads to a wider range of mass flow rate variation compared to varying the outlet pressure, primarily due to the corresponding changes in the density of the inlet fluid.

The turbine exhaust temperature is a critical limiting parameter at part load operation However, defining the maximum exhaust temperature for a particular design requires evaluating the operating temperatures and pressure ratios, in addition to defining the material limits and cooling system capabilities. Whilst this ensures a meaningful definition of the maximum exhaust temperature for a specific design, it is difficult to define this for turbine designs considered in this study. Therefore, to simplify the analysis, the limit of off-design operating conditions in this study is considered the minimum acceptable turbine efficiency. In this regard, an arbitrary total-to-total efficiency of 70% is selected to provide the base for the comparison and allow for the evaluation of the sensitivity of turbine aerodynamic performance to different design parameters. This value is approximately equal to the total-to-total efficiency at half-load in terms of mass flow rate of the reference 4-stage model. It is worth noting that efficiency limit other than 70% can be used to identify the turbine operating range at off-design. That should result in similar trends as the performance curves do not intersect as shown in Figure 5 and Figures 7-10.

Number of stages

The effect of varying the number of stages on the off-design performance is shown in Figure 7. It can be seen from the figure that the larger the number of stages, the higher the efficiency at both design and off-design operating conditions if all other flow path design parameters are kept the same. It can be seen from the figure that increasing the number of stages from 4 to 9 increases the total-to-total efficiency by 6.25% while increasing the number of stages from 8 to 14 stages further improves the efficiency by 0.7%. Similar observations are made from mean line design calculations adopting the Aungier loss model, as reported by Salah et al. [20], where the total-to-total efficiency gain is 4.8% when the number of stages is increased from 4 to 14. The minimum mass flow ratios, defined as the ratio between the mass flow rate to the design mass flow rate, at part-load for the 4, 9, and 14 stages are 41.8%, 43.7%, and 48%, respectively. Thus, increasing the number of stages from 4 to 14 increases the range of part-load mass flow rates by 6.2%.

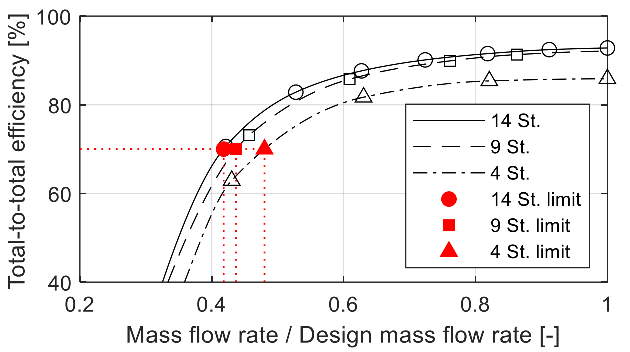

Figure 7 Effect of the number of stages on the off-design efficiency against the mass flow rate ratio to the design mass flow rate.

It can also be observed from Figure 7 that the differences between the three designs in terms of the total-to-total efficiency remain consistent across different mass flow rate ratios. For a mass flow rate ratio of 60%, the total-to-total efficiency obtained for the 14-stage, 9-stage, and 4-stage designs is 86.34%, 85.03%, and 78.87%, respectively. These values correspond a drop in efficiency of 6.5%, 7.1%, and 7.0% when compared to the efficiency at the design point, respectively. This consistency can be attributed to the similar operating conditions and design assumptions for the three models, which resulted in identical relation between the total-to-total pressure ratio and mass flow rate, irrespective of the number of stages, as shown in Figure 8.

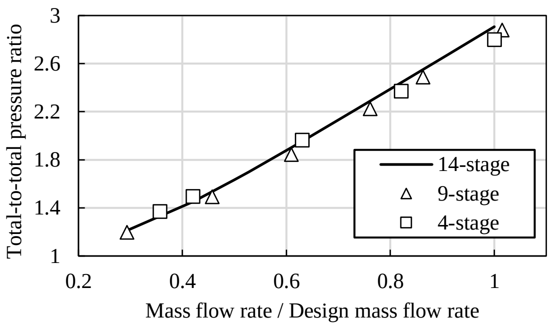

Figure 8 Relation between the mass flow rate ratio to the design mass flow rate and the total-to-total pressure ratio.

It is worth noting that all designs are based on the same flow coefficient and loading coefficient, which are set to values of 0.5 and 1, respectively during the mean line design. Decreasing the number of stages results in a significant performance deterioration at both design and off-design operating conditions because the enthalpy drop per stage, and hence the blade linear velocity, increases to maintain a constant loading coefficient. The higher blade velocity requires a larger hub diameter as the rotational speed is fixed for this application, and increasing the hub diameter decreases the blade aspect ratio and results in higher endwall losses. Furthermore, increasing the hub diameter increases the tip diameter and the tip clearance gap, resulting in higher tip leakage losses. These two loss components cause the observed performance deterioration for a lower number of stages, despite the flow and loading coefficients being set to the optimum values identified by the Smith chart.

Stator/rotor axial gap

The results of varying the stator/rotor axial gap are reported in Figure 9. It can be seen from the figure that increasing the axial gap from 33% to 50% of the downstream blade pitch length has a negligible effect at the design point and a minor effect at off-design. However, decreasing the stator/rotor axial gap from 33% to 15% has significantly decreased the performance and increased the aerodynamic losses at both design and off-design operating conditions. This could be attributed to the mixing losses developed in the axial gap between the stator and rotor domains. These losses increase when the axial distance downstream of the trailing edge is insufficient for the trailing edge wakes to disperse before approaching the following blade row. In this regard, the mixing losses are evaluated for the 15% and 50% axial gaps at both design and off-design by evaluating the entropy difference across the axial gap, as summarised in Table 3. It can be seen from the table that decreasing the axial gap increases the mixing losses relative to the stage losses. It can also be seen from the table that decreasing the axial gap from 50% to 15% results in an increase in the mixing losses from 19.1% to 37.7% at the design point and from 17.9% to 36.1% at off-design.

By analysing the results shown in Figure 9, a considerable sensitivity is observed in the minimum acceptable part-load mass flow ratio to the axial gap. The variation in the minimum mass flow ratio between the different axial gaps is found to be around 5.6%. Based on the obtained performance predictions, it is advisable to set the axial gap to pitch ratio to be above 33% although this would increase the turbine bearing span and decrease the rotor dynamic stability. A compromise between efficiency and mechanical assessment should be made in this regard.

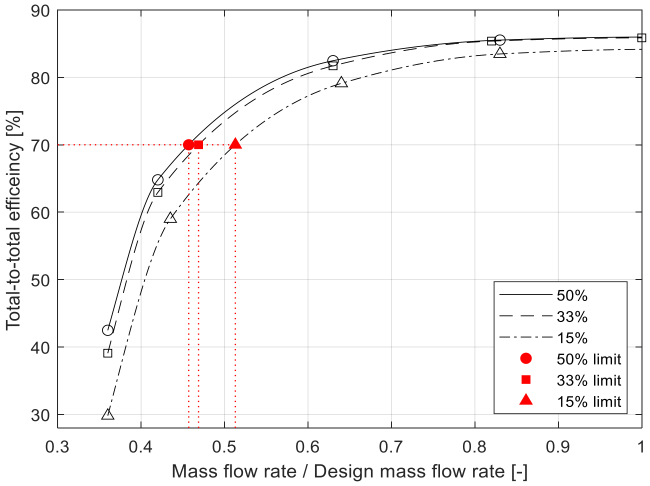

Figure 9 Effect of changing the stator/rotor axial gap on the off-design performance of the 4-stage sCO_2-SO_2 turbines.

Table 3 Entropy rise across the turbine and the mixing planes at both design and off-design for two different stator/rotor axial gap models.

	Design point		Off-design ($\dot{m}/\dot{m}_d \approx$ 63%)	
	50%	**15%**	**50%**	**15%**
$\Delta s_{Turbine}$ [J/kg.K]	25.96	29.24	18.35	21.79
Δs_{Mixing} [J/kg.K]	4.96	11.02	3.29	7.86
Mixing losses [%]	19.1%	37.7%	17.9%	36.1%

Aerofoil thickness near the leading-edge

The effect of varying the leading-edge thickness is shown in Figure 10. A constant leading-edge thickness is applied to all the blade rows of the 14-stage design, specifically, 2.5 mm, 3.5 mm, and 6 mm. Additionally, a variable leading-edge thickness is incorporated, where it is set to 20% of the chord length. Assuming a fixed percentage results in an increase in the leading-edge thickness as the chord length increases with the stage number. The results indicate that changes in the leading-edge thickness have minimal impact on the performance curve. A change in the leading-edge thickness from 2.5 mm to 6 mm corresponds to a change in the range of minimum acceptable mass flow ratios of 0.6%. Having said this, increasing the LE thickness does have a small positive impact on the off-design performance, but this corresponds to a reduction in the efficiency at the design point. Specifically, there is a slight decrease of approximately 0.3 pp in the total-to-total efficiency at the design point. This decrease in efficiency can be attributed to the increased profile losses resulting from the thicker leading-edge. However, it is worth noting that this efficiency drop is relatively minor since the flow remains well-attached to the blades across the investigated range of leading-edge thicknesses.

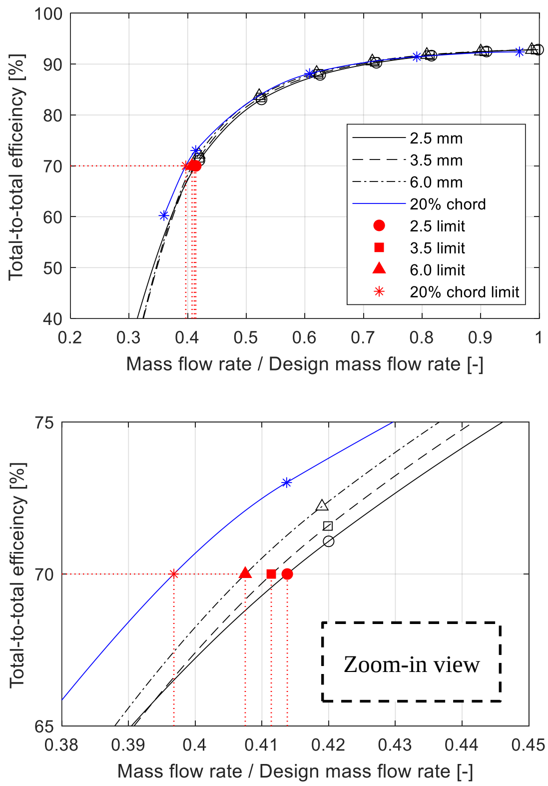

Figure 10 Effect of changing the leading-edge thickness on the off-design performance of the 14-stage sCO_2-SO_2 turbines. Top figure (Full range), and bottom figure (zoom-in view).

A further improvement in the off-design performance is found when defining the leading-edge thickness as 20% of the blade chord length. For this design, the leading-edge thickness varies between 8.7 mm, and 13.2 mm, corresponding to a variation in the chord length from 43 mm to 66 mm, respectively. The drop in total-to-total efficiency at the design point in this case is 0.44 percentage points (pp) relative to the reference model with the leading-edge thickness of 2 mm. This minor change shows that the flow remains attached to the walls at the design point. The achieved reduction in mass flow ratio at part-load is increased to 1.7%. It is observed that increasing the leading-edge thickness decreases the flow separation regions that develop near the pressure side of the blade, leading to reduced incidence losses at off-design operating conditions. Although this improvement is observed, it is relatively small compared to the improvements achieved by increasing the number of stages or increasing the stator/rotor axial gap.

Modifying the blade inlet wedge angle within the range of 5° to 25° yields a comparable effect to adjusting the thickness of the leading-edge, with minimal impact on the off-design performance, as shown in Figure 11. Within this range, the minimum part-load mass flow rate varies by 2% of the design mass flow rate, with a negligible effect on the design point efficiency. The flow field results have shown that no flow separation is experienced due to increasing the leading-edge thickness at the design point. In addition, no significant changes were observed in the other sources of loss due to varying the blade thickness near the leading-edge at the design point.

Increasing the blade thickness, achieved by increasing the inlet wedge angle, contributes to decreasing the separation regions at part-load operating conditions. This positive effect is achieved by utilising the extra blade thickness to partially fill the separation region while ensuring that the outlet flow angles and throat openings remain unaffected. As a result, the downstream stages are not impacted by this modification.

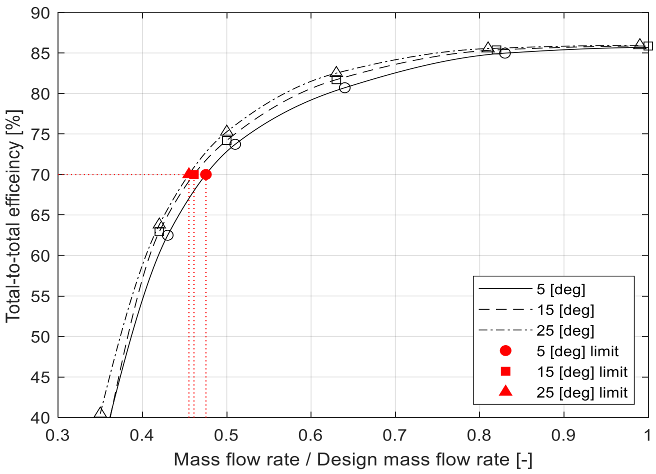

Figure 11 Effect of changing the inlet wedge angle on the off-design performance of the 4-stage sCO_2-SO_2 turbines. The top figure shows the full range, and the bottom figure shows a zoom-in view.

Stagger Angle

The effect of varying the stagger angle on the off-design performance of the 4-stage design is shown in Figure 12. The 4-stage model is selected for simplicity, although similar trends are observed for a different number of stages. The stagger angles are varied between -10° to +5° relative to the design values with a step of 5°.

It can be seen from the figure that at the design point, a slight improvement in the total-to-total efficiency of around 0.9% is observed by increasing the stagger angle by 5° compared to the reference design. This can be attributed to the uncertainty of the reference design conducted using the Aungier mean line loss model. Previous investigations of similar turbines showed that the difference between the total-to-total efficiency estimated by the Aungier loss model and the CFD model at the design point is around 1.01 percentage points (pp) [23]. In addition, the blade stresses are calculated as a function of the blade stagger angle in the mean line model and the stress limits were set based on practical recommendations to ensure the safety of the proposed design by Salah [26]. These preliminary design assumptions may have led to more conservative values of the stagger angle, sacrificing the performance to satisfy the bending stress limits.

At off-design operating conditions, the off-design performance is significantly improved when the stagger angle is increased. The achieved improvement in the mass flow rate range is 6.63% relative to the design values. By decreasing the stagger angle, the performance at both design and off-design deteriorates, where the minimum achievable mass flow ratio for the -10° case is 74.6% compared to 46.3% at the design point.

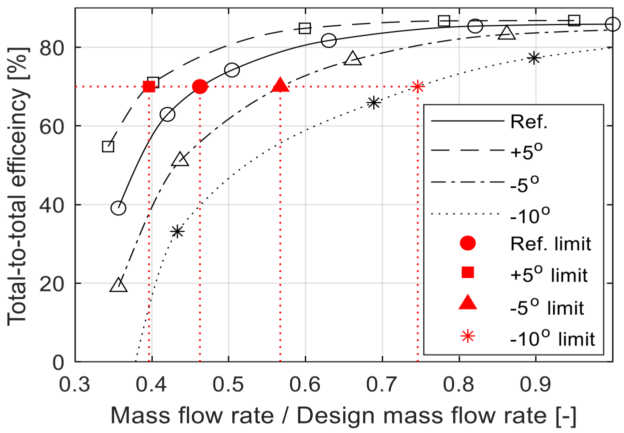

Figure 12 Effect of the stagger angle on the off-design performance.

To further understand the performance improvement achieved by increasing the stagger angle, the relative Mach number distribution is compared with the reference stagger angle at design and off-design operating conditions. The results for the design point (DP), as well as two off-design total-to-static pressure ratios, specifically 1.83, and 1.37, are presented in Figure 13. It can be seen from the figure that increasing the stagger angle has a negligible impact at the design point. However, the significance of increasing the stagger angle becomes apparent at off-design conditions where flow separation occurs. For off-design operating conditions, increasing the stagger angle decreases the flow separation region. Consequently, the incidence and profile losses both decrease, and the overall stage performance is improved.

It should be noted that changing the stagger angle may affect the throat opening of the blades as shown in Figure 14. The resulting change in the mass flow rate corresponding to the change in the stagger angle is shown in Figure 15. Increasing the stagger angle from -5° to +5° relative to the design values resulted in a change in the mass flow ratio of 10.2% near the design operating conditions and around 3.6% at half-load. This is linked to decreasing the average throat opening per stage from 16.2 mm to 17.5 mm corresponding to the changing the stagger angle from -5° to +5°, respectively. This corresponds to a decrease in the throat opening of 8% relative to the design value.

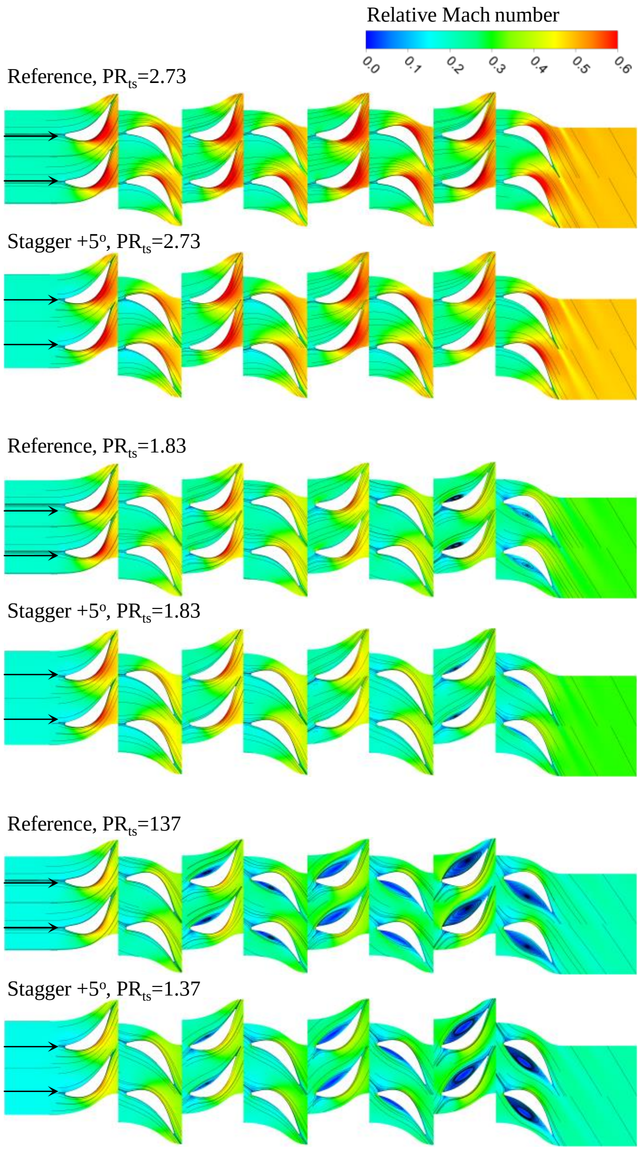

Figure 13 The effect of increasing the stagger angle on the flow structure, at different operating conditions. (DP: design point).

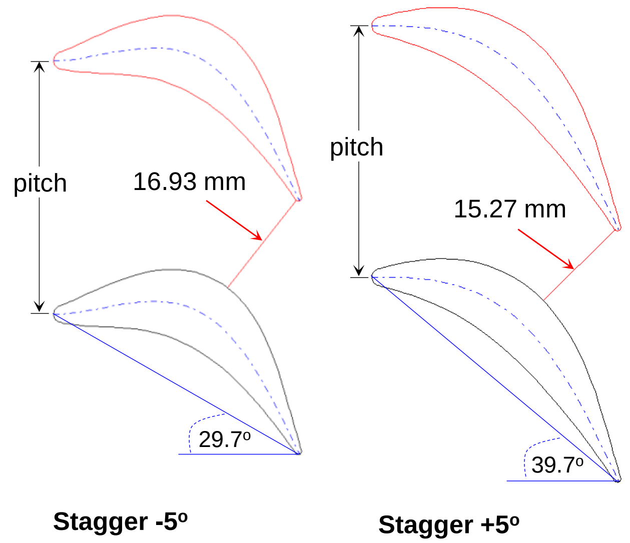

Figure 14 Change in the throat opening corresponding to the change in the stagger angle.

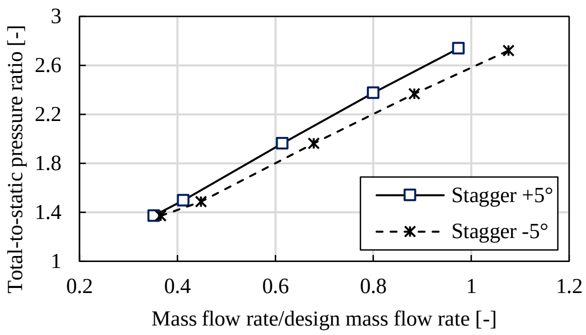

Figure 15 The effect of changing the stagger angle on the mass flow ratio calculated at +/-5° from the reference stagger angle.

It is worth noting that the geometrical changes made to both the stagger angle and the inlet wedge angles are applied to all the turbine stages. This approach is followed because of two main reasons. Firstly, the number of stages affected by flow separation is variable with the mass flow rate. Secondly, applying these modifications to the stages that are not affected by boundary layer separation has no significant impact on the stage performance. Therefore, increasing the stagger angle or the inlet wedge angle for all the turbine stages offers a better performance over a wider range of operation at part-load. In addition, increasing the stagger or inlet wedge angles of the first stages does not add risk to the mechanical design of the blades, as these stages have shorter blades and are not critical when considering bending stresses.

Increasing the stagger angle has a negative impact on the blade bending stresses as the blade axial chord decreases and the tangential chord increases. In this case, the blade aerofoil geometry tends to be closer to the direction normal to the axis of the turbine leading to higher blade loading. In this regard, the sensitivity of the maximum equivalent bending stress to the stagger angle is analysed to understand the consequences of the achieved aerodynamic performance enhancement.

The von Mises stresses on the last rotor blade of the 4-stage design are evaluated using the FEA model for the reference stagger angle and for the +5° stagger angle design at the design point operating condition, as shown in Figure 16. It is worth noting that the bending stresses that arise due to the pressure difference across the blade are decreased at part-load due to the reduction in the pressure drop per stage; as such, stresses are expected to be at a maximum at full load operating condition. It can be seen from the figure that increasing the stagger angle by 5° resulted in an increase in the peak stress of 11.1 MPa which is approximately 7.2% of the reference peak stress value. Although the stress increase is not significant in this case, since the peak stress for reference design was not close to the maximum, for designs with a large number of stages the peak stresses could be closer to the stress limit margin. Increases in peak stresses could be mitigated by increasing the blade base fillet radius, the blade thickness at the base profile, or increasing the blade chord length to maintain it within the acceptable limits. As such, changes to the stagger angle should be carefully evaluated and possible mitigation measures implemented.

Comparing the impact of the geometrical adjustments

The sensitivity of the minimum allowable mass flow ratio to the various design parameters considered in this study is summarised in Figure 17. This analysis involves evaluating the minimum acceptable mass flow ratio at the extreme boundaries of each design variable and evaluating the range of the minimum acceptable mass flow ratio corresponding to these limits.

It has been found that the stagger angle has the largest effect on performance, with a 17.1% change in the mass flow ratio, corresponding to a variation in the stagger angle ±5°. The leading-edge thickness has shown the least impact on the minimum acceptable mass flow rate with a 0.63% change corresponding to a change in the leading edge thickness between 2.5 mm and 6 mm. Both the number of stages and the stator/rotor axial gap have a considerable effect on the off-design performance, however, the relation between these parameters and the turndown capability is not linear. For example, increasing the number of stages from 9 to 14 has less influence on performance improvement compared to increasing the number of stages from 4 to 9. Similarly, increasing the axial gap from 33% to 50% is less effective than increasing it from 15% to 30% of the pitch length.

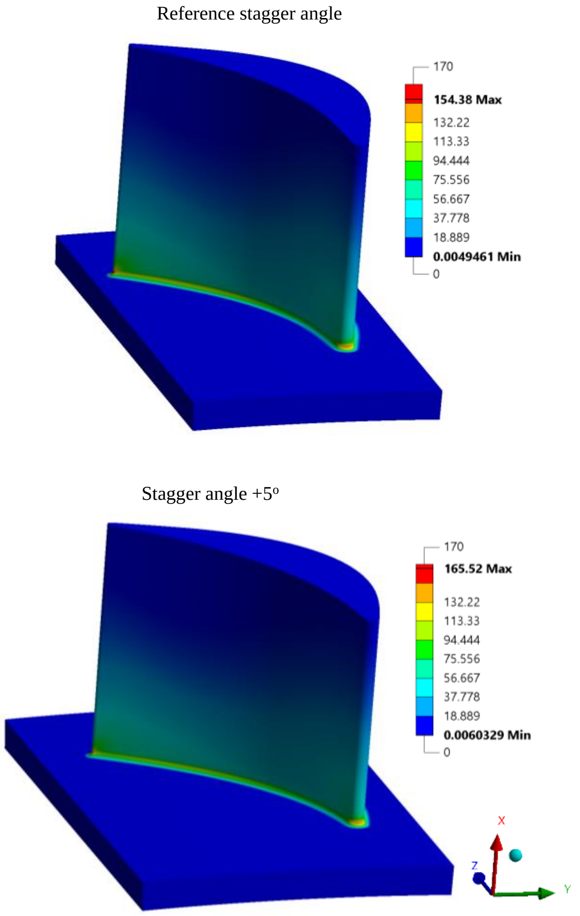

Figure 16 Stress distribution obtained for the last stage rotor of the 4-stage design for the reference and modified stagger angles (+5º).

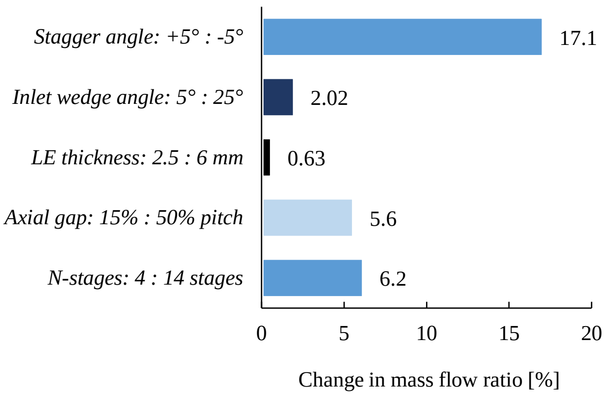

Figure 17 Sensitivity of the minimum part-load mass flow ratio to the different flow path design parameters.

CONCLUSION

Off-design performance analysis of turbomachinery is important for evaluating cycle efficiency of a given power plant at various operating conditions. The off-design performance of large-scale axial turbines operating with a CO_2-SO_2 mixture has been investigated using steady-state Reynolds averaged Navier-Stokes flow simulations. The findings of this paper include the quantification of the impact of different turbine design parameters, including the number of stages, stagger angle, rotor/stator axial spacing and leading-edge thickness, on the design and off-design performance of the turbine. This information can aid in the future design of turbines operating supercritical CO_2 power cycles, with high efficiency across a range of operating conditions.

A 3D multi-stage CFD model was setup and verified against a small-scale air turbine, demonstrating good agreement with both experimental and numerical data. A uniform deviation in total-to-static efficiency was observed compared to the published experimental and numerical results of 1.7%, and 2.9%, respectively, at both design and part-load operating conditions.

A parametric study considering the effect of different blade design parameters on off-design performance has revealed that of the parameters investigated the stagger angle has the largest influence on both design and off-design performance. By increasing the stagger angle from -5º to +5º from the reference angle, the minimum acceptable mass flow rate is decreased by 17.1% compared to the design value. This increase in the stagger angle resulted in an increase in the design point total-to-total efficiency of 2.3 percentage points. On the other hand, the leading-edge thickness has shown the least influence with 0.63% change in the minimum part-load mass flow ratio with a negligible effect on the design point efficiency. Both the number of stages and the stator/rotor axial gap have a more considerable effect on off-design performance with a variation in the mass flow ratio of 6.2% and 5.6%, respectively.

Increasing the number of stages has been found to be beneficial at both design and off-design operating conditions. The performance improvement achieved by increasing the axial gap from 15% to 50% of the pitch can be attributed to a decrease in mixing losses from 37% to 19% of the total stage losses at the design point. The flow field investigations have revealed that the performance enhancement obtained by increasing the inlet wedge angle, leading-edge thickness, and stagger angle can be attributed to the reduction in separation regions by mitigating the impact of high incidence angles, particularly in the final turbine stages. However, it should be noted that increasing the stagger angle, while improving performance, may lead to increased bending stresses. For instance, when the stagger angle was increased from the reference value to +5°, the bending stresses experienced under the design point increased by 7.2%.

Ultimately, enhancing the performance at both design and off-design operating conditions can be achieved by increasing the number of stages, increasing the stagger angle, and increasing the stator/rotor axial gap. However, increasing the blade thickness near the leading-edge can improve off-design performance while negatively impacting the design point efficiency. These parameters should be carefully adjusted to satisfy bending stress and rotor dynamic constraints.

REFERENCES

[1] White, M. T., Bianchi, G., Chai, L., Tassou, S. A., and Sayma, A. I., 2021, "Review of supercritical CO_2 technologies and systems for power generation," *Applied Thermal Engineering*, 185, p. 116447. 10.1016/j.applthermaleng.2020.116447

[2] Crespi, F., de Arriba, P. R., Sánchez, D., and Muñoz, A., 2022, "Preliminary investigation on the adoption of CO_2-SO_2 working mixtures in a transcritical Recompression cycle," *Applied Thermal*

Engineering, 211, p. 118384. 10.1016/j.applthermaleng.2022.118384

[3] Lasala, S., Bonalumi, D., Macchi, E., Privat, R., and Jaubert, J. N., 2017, "The design of CO_2-based working fluids for high-temperature heat source power cycles," *Energy Procedia*, 129, pp. 947-954. 10.1016/j.egypro.2017.09.125

[4] Vance, J. M., Zeidan, F. Y., and Murphy, B. G., 2010, Machinery vibration and rotordynamics, Chapter No. 6, *John Wiley & Sons*.

[5] Abdeldayem, A., Salah, S., White, M., and Sayma, A., 2023, "A modified loss breakdown approach for axial turbines operating with blended supercritical carbon dioxide," *Journal of Engineering for Gas Turbine and Power*, 145(8), p. 081002. 10.1115/1.4062478

[6] Zhang, H., Zhao, H., Deng, Q., and Feng, Z., 2015, "Aerothermodynamic design and numerical investigation of supercritical carbon dioxide turbine," *Proc. Turbo Expo: Power for Land, Sea, and Air*, American Society of Mechanical Engineers, p. V009T036A007. 10.1115/GT2015-42619

[7] Shi, D., Zhang, L., Xie, Y., and Zhang, D., 2019, "Aerodynamic design and off-design performance analysis of a multi-stage S-CO_2 axial turbine based on solar power generation system," *Applied Sciences*, 9(4), p. 714. 10.3390/app9040714

[8] Moustapha, S., Kacker, S., and Tremblay, B., 1990, "An improved incidence losses prediction method for turbine airfoils," *Journal of Turbomachinery*, 112(2), pp. 267-276. 10.1115/1.2927647

[9] Hamakhan, I. A., and Korakianitis, T., 2010, "Aerodynamic performance effects of leading-edge geometry in gas-turbine blades," *Applied Energy*, 87(5), pp. 1591-1601. 10.1016/j.apenergy.2009.09.017

[10] Benner, M. W., Sjolander, S. A., and Moustapha, S. H., 1997, "Influence of Leading-Edge Geometry on Profile Losses in Turbines at Off-Design Incidence: Experimental Results and an Improved Correlation," *Journal of Turbomachinery*, 119(2), pp. 193-200. 10.1115/1.2841101

[11] Dossena, V., D'Ippolito, G., and Pesatori, E., 2004, "Stagger Angle and Pitch-Chord Ratio Effects on Secondary Flows Downstream of a Turbine Cascade at Several Off-Design Conditions," *Proc. ASME Turbo Expo 2004: Power for Land, Sea, and Air*, pp. 1429-1437. 10.1115/gt2004-54083

[12] Salah, S. I., White, M. T., and Sayma, A. I., 2022, "A comparison of axial turbine loss models for air, sCO_2 and ORC turbines across a range of scales," *International Journal of Thermofluids*, p. 100156. 10.1016/j.ijft.2022.100156

[13] Vogt, D. M., and Fransson, T. H., 2006, "Experimental Investigation of Mode Shape Sensitivity of an Oscillating Low-Pressure Turbine Cascade at Design and Off-Design Conditions," *Journal of Engineering for Gas Turbines and Power*, 129(2), pp. 530-541. 10.1115/1.2436567

[14] Du, Y., Chen, K., and Dai, Y., 2019, "A study of the optimal control approach for a Kalina cycle system using a radial-inflow turbine with variable nozzles at off-design conditions," *Applied Thermal Engineering*, 149, pp. 1008-1022. 10.1016/j.applthermaleng.2018.12.117

[15] Benner, M. W., Sjolander, S. A., and Moustapha, S. H., "Influence of Leading-Edge Geometry on Profile Losses in Turbines at Off-Design Incidence: Experimental Results and an Improved Correlation," *Proc. ASME 1995 International Gas Turbine and Aeroengine Congress and Exposition*V001T01A075. 10.1115/95-gt-289

[16] Jang, H. J., Kang, S. Y., Lee, J. J., Kim, T. S., and Park, S. J., 2015, "Performance analysis of a multi-stage ultra-supercritical steam turbine using computational fluid dynamics," *Applied Thermal Engineering*, 87, pp. 352-361. 10.1016/j.applthermaleng.2015.05.007

[17] Aqel, O., White, M., and Sayma, A., "Binary interaction uncertainty in the optimisation of a transcritical cycle: consequences on cycle and turbine design," *Proc. 4th European sCO_2 Conference for Energy Systems: March 23-24, 2021, Online Conference*, pp. 164-176. 10.17185/duepublico/73942

[18] Aqel, O. A., White, M. T., Khader, M., and Sayma, A., 2021, "Sensitivity of transcritical cycle and turbine design to dopant fraction in CO_2-based working fluids," *Applied Thermal Engineering*, 190, p. 116796. 10.1016/j.applthermaleng.2021.116796

[19] Crespi, F. M., Rodriguez de Arriba, P., Sánchez Martínez, D. T., Ayub, A., Di Marcoberardino, G., Invernizzi, C. M., Sánchez Martínez, G., Iora, P., Di Bona, D., Binotti, M., and Monzolini, G., 2022, "Thermal efficiency gains enabled by using CO_2 mixtures in supercritical power cycles," *Energy*, 238, p. 121899. 10.1016/j.energy.2021.121899

[20] Salah, S. I., Crespi, F., White, M. T., Muñoz, A., Paggini, A., Ruggiero, M., Sánchez, D., and Sayma, A. I., 2023, "Axial turbine flow path design for concentrated solar power plants operating with CO_2 blends," *Applied thermal engineering*, p. 120612. 10.1016/j.applthermaleng.2023.120612

[21] Abdeldayem, A., White, M., Paggini, A., Ruggiero, M., and Sayma, A. I., 2022, "Integrated Aerodynamic and Structural Blade Shape Optimisation of Axial Turbines Operating with Supercritical Carbon Dioxide Blended with Dopants," *Journal of Engineering for Gas Turbine and Power*, 144(10), p. 101016. 10.1115/1.4055232

[22] Petrovic, M. V., and Riess, W., 1997, "Off-design flow analysis and performance prediction of axial turbines," *Proc. Turbo Expo: Power for Land, Sea, and Air*, American Society of Mechanical Engineers, p. V001T003A013. 10.1115/97-GT-055

[23] Abdeldayem, A., Salah, S., Aqel, O., White, M., and Sayma, A., 2023, "Design of a 130 MW axial turbine operating with a supercritical carbon dioxide mixture for the SCARABEUS project," *International Journal of Turbomachinery, Propulsion and Power*. 10.3390/ijtpp9010005

[24] Denton, J. D., 1993, "Loss mechanisms in turbomachines," *Journal of Turbomachinery*, 115(4), pp. 621-656. 10.1115/1.2929299

[25] Abdeldayem, A., Paggini, A., Diurno, T., Orazi, C., White, M., Ruggiero, M., and Sayma, A., 2023, "Integrated aerodynamic and mechanical design of a large-scale axial turbine operating with supercritical carbon dioxide mixtures," *Journal of Engineering for Gas Turbine and Power*. 10.1115/1.4063530

[26] Salah, S., 2023, "Design and analysis of supercritical carbon-dixoide axial turbines," *PhD Thesis, City, University of London*.